Structure and magnetic properties of Ni/Cu/Fe/MgO(001) films

2009 J. Phys.: Condens. Matter 21 156002

(http://iopscience.iop.org/0953-8984/21/15/156002)

J. Phys.: Condens. Matter **21** (2009) 156002 (6pp) doi:10.1088/0953-8984/21/15/156002

Structure and magnetic properties of Ni/Cu/Fe/MgO(001) films

G Lauhoff[1], C A F Vaz[2] and J A C Bland[3]

Cavendish Laboratory, Madingley Road, Cambridge CB3 0HE, UK

E-mail: georglauhoff@georglauhoff.com and carlos.vaz@cantab.net

Received 19 November 2008, in final form 25 February 2009
Published 20 March 2009
Online at stacks.iop.org/JPhysCM/21/156002

Abstract

The structural and magnetic properties of thin Ni films grown on Cu/Fe/MgO(001) and Cu/MgO(001) buffer layers are investigated and compared to those grown on Cu/Si(001). The use of an Fe seed layer a few monolayers thick leads to the epitaxial growth of high surface quality Cu(001) buffer layers on MgO(001), while Cu growth on the bare MgO(001) substrate results in polycrystalline films. Magneto-optic Kerr effect magnetometry shows that Ni films grown on Cu/Fe/MgO(001) exhibit dominant perpendicular magnetic anisotropy up to ∼90 Å, which is similar to that of Ni films grown on Cu/Si(001). The polycrystalline Ni films also exhibit perpendicular magnetic remanence, but with a dominant in-plane magnetization component.

(Some figures in this article are in colour only in the electronic version)

Since the first report of perpendicular magnetic anisotropy (PMA) by Gradmann and Müller [1, 2], several other thin films and multilayer systems have been shown to exhibit PMA. Among these, Ni/Cu(001) films are an interesting case: epitaxial Cu/Ni/Cu(001) thin films show PMA over a large thickness range from about 15–140 Å [3–8], which arises from the magneto-elastic anisotropy contribution due to the tensile strain induced by the lattice mismatch with the Cu(001) substrate. Ni films have been grown on Cu(001) single crystals, which offer the best film quality [8]; in other studies, Ni/Cu(001) have been grown epitaxially on Si(001) substrates [3–7], which has the advantage of ease of preparation and offers the possibility of integration with semiconductors (although reaction between Si and Cu remains an issue, see [9] and references therein). More recently, there has been wide interest in using metal oxides as key components for post-CMOS devices, and the recent demonstration of very large tunnel magnetoresistance ratios in Fe/MgO/Fe tunnel junctions [10–12] is but one example of the potential of metal oxides in magnetoelectronic devices. Here, we consider the structure and magnetic properties of Ni/Cu(001) epitaxial films grown on MgO(001) substrates by means of an Fe seed layer, which are compared to those of films grown on Si(001). Another motivation stems from the larger lattice mismatch between Cu and MgO (14%) as compared to the 5.6% mismatch between Cu and Si. Cu grown epitaxially on MgO may be expected to be strained to a larger extend compared to Cu grown on Si(001) and our purpose here is to investigate the effect of strain on the structure and magnetic properties of Ni(001) films grown on Cu/Fe/MgO(001).

It has been reported that Cu does not grow epitaxially at room temperature on MgO due to the large lattice mismatch between the layers and a weak film–substrate interaction [13, 14]. However several approaches have been studied to achieve epitaxial Cu/MgO(001), such as film deposition at elevated temperatures and by using seed layers. Yang and Perry [15] reported an increase in the island diameter of Cu grown on MgO(001) with increasing deposition temperature up to 650 K, at which point a continuous film ensues. Mewes *et al* [16] used Pt and Pt/Fe seed layers to achieve epitaxial growth of Cu on MgO(001): while for Cu/MgO(001) the film exhibit three-dimensional island growth, as found in other studies, the use of a Pt seed layer leads to the growth of [111]-oriented Cu films, whereas a 5 Å Fe/Pt seed layer results in Cu(001) epitaxy. In the present study, we report the growth of Cu(001) on MgO(001) by using a single Fe seed layer.

[1] Present address: Samsung Information Systems America, 75 West Plumeria Drive, San Jose, CA 95135, USA.
[2] Present address: Applied Physics, Yale University, New Haven, CT 06520, USA.
[3] Deceased.

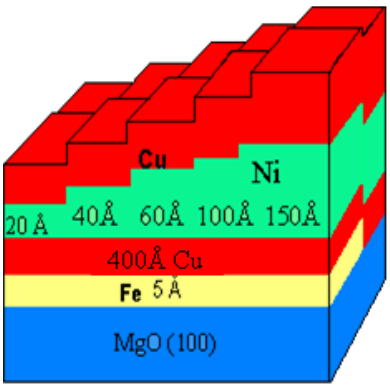

Figure 1. Schematic diagram of the sample structure. Actual lateral sample size is 1 × 1 cm^2.

Table 1. Film deposition condition.

	Deposition rate (Å min^{-1})	Temperature (°C)	Pressure during growth (mbar)
Fe seed layer (5 Å)	10	∼450	$<6 \times 10^{-9}$
Cu buffer layer (400 Å)	10	∼100	$<9 \times 10^{-9}$
Ni layer (20–150 Å)	1.7	Ambient	$<9 \times 10^{-10}$
Cu capping layer (50 Å)	10	Ambient	$<4 \times 10^{-9}$
Au layer (30 Å)	60	Ambient	$<7 \times 10^{-9}$

1. Experimental details

The MgO(001) substrate was firstly cleaned in isopropyl alcohol (IPA) followed by an oxygen plasma etched for 1 min at 10^{-1} mbar oxygen gas pressure. The substrate was then inserted into the load-lock of the ultra-high vacuum deposition chamber within ∼10 min after cleaning. After an overnight bake-out, the MgO(001) substrate was annealed for 3 h at 270 °C with a base pressure of 4×10^{-10} mbar. A similar cleaning process of the MgO substrate has been reported by Mewes *et al* [16]. Metal deposition was carried out under UHV by e-beam heating of the target material. The conditions (pressure, temperature and growth rate) for each stage of the growth are shown in table 1. After completion of the film deposition, the cleanliness of the films was ascertained by Auger electron spectroscopy (AES) while sample crystallinity was determined by reflection high energy electron diffraction (RHEED) using a beam energy of 15 keV.

Figure 1 shows a schematic diagram of the staircase structure prepared for this study. It consists of a Ni staircase layer (20, 40, 60, 100, and 150 Å), half of which is grown onto Cu/Fe/MgO(001) while the other half is grown directly onto 400 Å Cu/MgO(001), without the 5 Å Fe seed layer. For the growth of the Fe and Ni staircase films a shutter close to the sample was used. While the shutter is fixed at a certain position, the sample can be translated or rotated with a micrometer stage, which allows accurate control for the growth

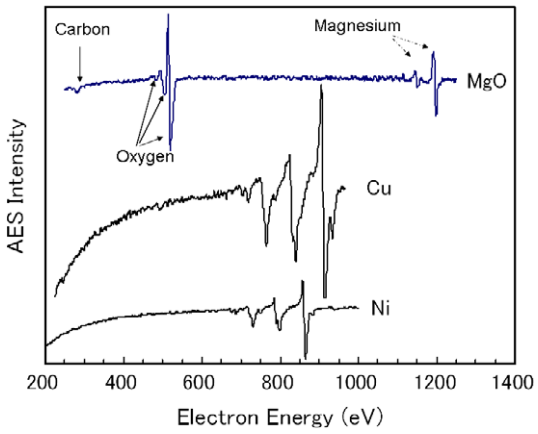

Figure 2. Auger electron spectroscopy scans for the MgO substrate (top), the 400 Å Cu buffer layer (middle), and after the completion of the Ni film (bottom).

of the staircase. The step width is 2 mm for the Ni staircase, while the sharpness of the step edge is estimated to be smaller than 0.1 mm. A 50 Å Cu film was then deposited onto the Ni layer, and the whole structure was finally capped by 30 Å Au to protect the sample from oxidation during the *ex situ* measurements. The film thicknesses were estimated using a calibrated quartz crystal monitor close to the sample position. We note that adjacent steps can be distinguished by the naked eye, allowing easy optical alignment in the magneto-optical measurements. The ability to translate or rotate the sample in the deposition system allows one to carry out RHEED and AES *in situ* on the different steps of the sample.

Magnetic hysteresis curves were measured at the different sample staircase positions using a magneto-optic Kerr effect (MOKE) magnetometer employing a focused HeNe laser with an approximate spot size of 0.2 mm. Measurements were carried out in two orientations, polar and longitudinal [17, 18]. In the polar configuration, both the external field and the incident laser beam are perpendicular to the sample surface, so that only the perpendicular component of the magnetization is measured. In the longitudinal MOKE configuration, the applied field direction was parallel to the sample surface and the laser beam was incident at ∼30° with respect to the surface normal; in this configuration MOKE is sensitive to both perpendicular and in-plane components of the magnetization. One feature (and advantage) of using MOKE in this study is the limited probing depth (around 200 Å at the HeNe laser wavelength, $\lambda = 633$ nm): the Ni film was grown onto a 400 Å Cu/Fe/MgO(001) and the Cu film thickness is larger than the probing depth of the light. Therefore, only the Ni layer is detected in our MOKE measurements. In addition, we also expect the magnetic interaction between the Fe and Ni films to be negligible, since the stray field issuing from the Fe film is small (scaling as thickness/width) and since a 5 Å (∼2 ML) Fe/MgO(001) is expected to be superparamagnetic at remanence [19].

2. Experimental results

Figure 2 shows the AES spectra for the MgO substrate prior to film growth (top), after completion of the 400 Å Cu film

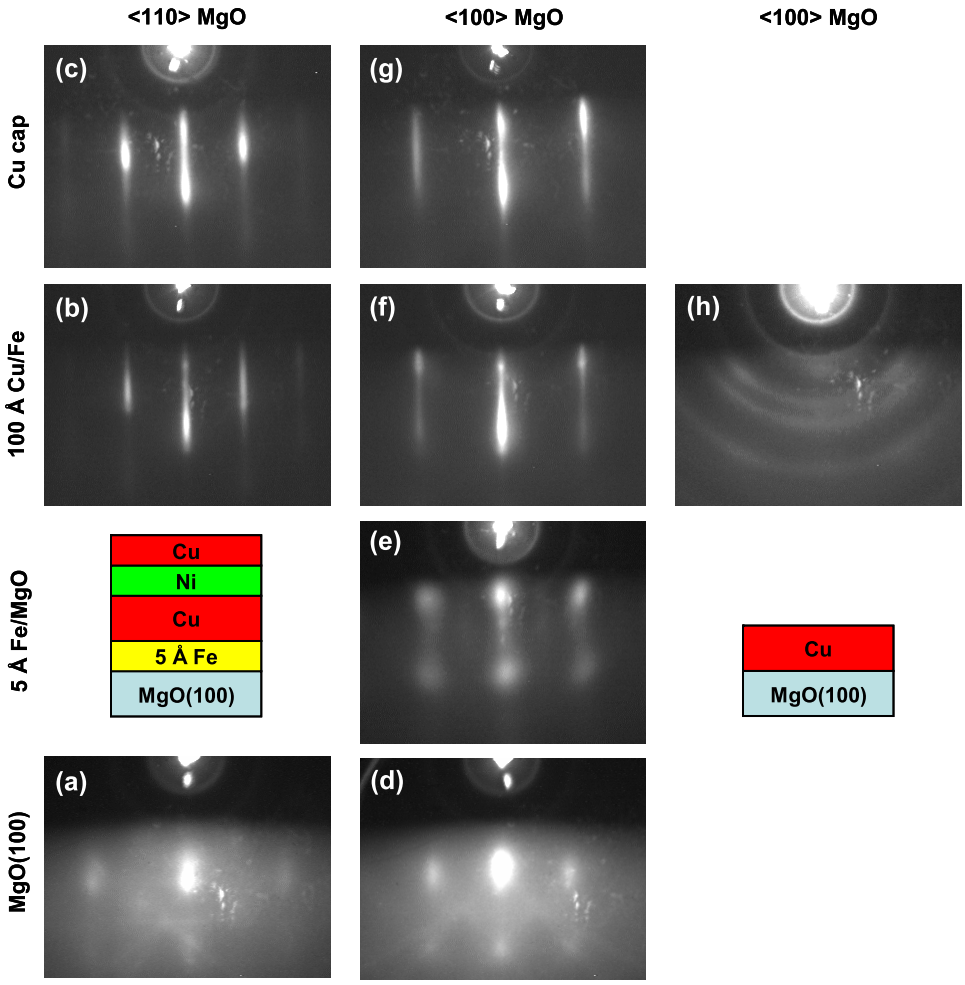

Figure 3. RHEED images for (a)–(g) Cu/Ni/Cu/Fe/MgO(001) and (h) the Cu film grown directly on MgO(001), during the sample growth.

(middle) and of the Ni film after growth (bottom). For the MgO substrate, the data show the Auger KLL Mg and O lines as well as a small C peak, indicating a small amount of C contamination. The Cu and Ni films show no traces of contaminants, to within the experimental resolution of our system (of ∼1.5%).

Figure 3 shows typical RHEED images taken at different stages of the sample growth along the MgO(001) ⟨110⟩ (left panels, (a)–(c)) and ⟨100⟩ (middle panels, (d)–(g)) azimuths for the Cu/Ni/Cu/Fe/MgO(001) structure, and along the MgO(001) ⟨100⟩ azimuth for the Cu/MgO(001) film (right panel, (h)). In the latter case, the Cu film and consecutive Ni and Cu layers grow polycrystalline, as indicated by the ring pattern (h). However, by using a 5 Å Fe seed layer, epitaxial growth of the Fe, Cu, Ni and Cu cap layers is achieved. The RHEED patterns indicate that the Fe seed layer (001) plane is rotated by 45° with respect to the MgO(001), which provides a better lattice match between the Fe and the MgO lattices [20]; the relative crystalline film orientation is given by: Ni(001)/Cu(001)[100] ∥ Fe(001)[110] ∥ MgO(001)[100]. The RHEED diffraction spots of the Fe layer are relatively broad, indicating some surface roughness; we also note a slight increase in the distance between the diffraction spots from the MgO to Fe to Cu, which suggest a progressive lattice relaxation of the crystal lattice of Fe [21] and Cu. Given the large lattice mismatch between Cu and Fe, $\eta^{\mathrm{Cu/Fe}} = (a^{\mathrm{Fe}} - a^{\mathrm{Cu}})/a^{\mathrm{Cu}}$ of about 12%, we suggest that most strain relaxation occurs over a very small interfacial region near the Fe seed layer that helps the Cu surface attain the equilibrium lattice constant at much lower thicknesses than for Cu buffer layers grown on Si(001).

Figure 4 shows a comparison of the RHEED patterns along the Cu(001) ⟨100⟩ azimuth for Cu buffer layers, 100 and 400 Å thick grown on Fe(5 Å)/MgO(001) (top panel) and 600, 2000 Å thick grown on Si(001) (bottom), taken from our earlier work [22, 23]. For the latter system, the RHEED patterns for the 2000 Å Cu film were found to be sharper and have a lower background compared to the images for the 600 Å Cu/Si(001), indicating that the 2000 Å thick Cu film has a better crystal quality (i.e., smaller surface roughness amplitude and larger in-plane coherence length) compared to the thinner Cu film; in addition, the in-plane lattice parameter was fully relaxed for the thicker Cu film. In comparison, while the RHEED patterns for 100 and 400 Å Cu grown on Fe/MgO(001) look qualitatively similar to each other (becoming slightly more streaky for the thicker (400 Å) Cu film), both patterns are much sharper than the 600 and 2000 Å Cu films grown on Si(001). This indicates that the surface is smoother for the Cu/Fe/MgO(001) than the Cu/Si(001), i.e., the Cu(001) films exhibit a much better

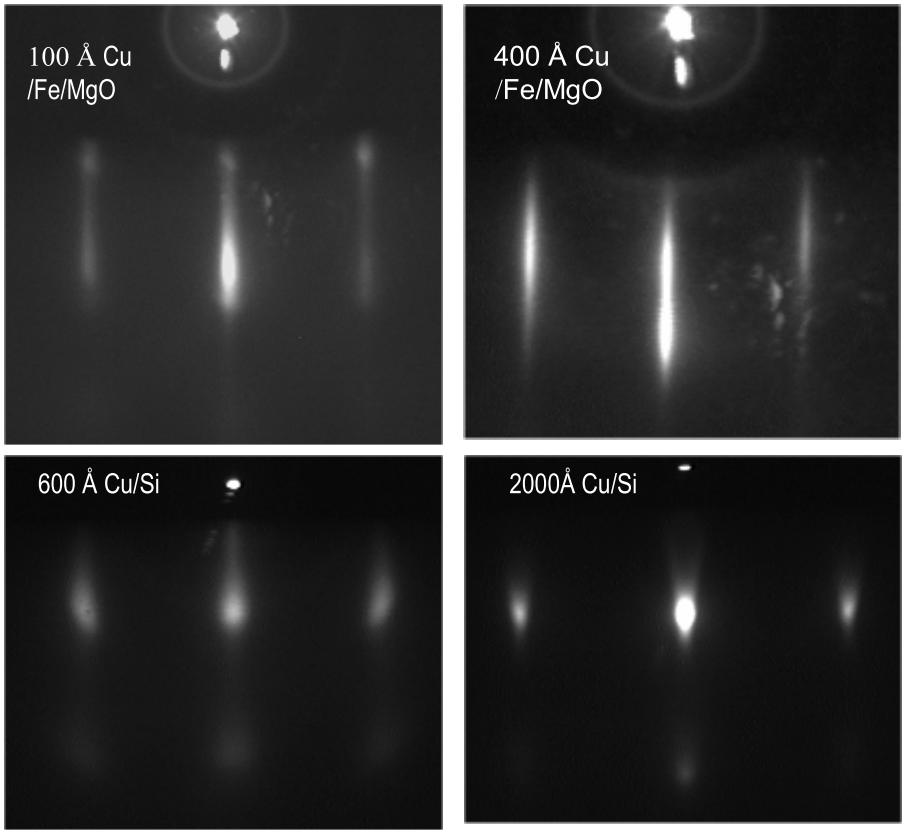

Figure 4. RHEED images for different Cu buffer layer thicknesses on Fe(5 Å)/MgO(001) (top) and on Si(001) (bottom).

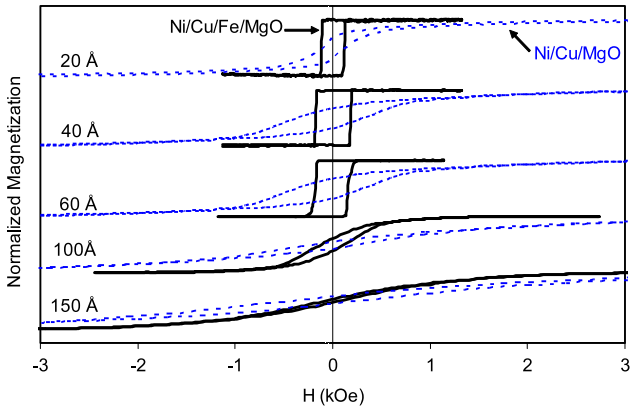

Figure 5. Normalized magnetization as determined from polar MOKE curves for Cu/Ni/Cu/Fe/MgO (straight black line) and Cu/Ni/Cu/MgO (blue dotted line) for the different Ni thicknesses.

surface crystal quality when grown on Fe/MgO compared to Si(001) at smaller, or comparable Cu thicknesses, despite the much larger lattice mismatch in the case of MgO(001).

Figure 5 shows the polar MOKE measurements for the epitaxial Cu/Ni/Cu/Fe/MgO (full line) and for the polycrystalline Cu/Ni/Cu/MgO(001) (dotted line) for the different Ni film thicknesses. The hysteresis curves show a much higher squareness and lower saturation field (characteristic of magnetization reversal by domain wall motion), and therefore larger PMA, for the epitaxial Ni films grown using the Fe seed layer compared to the polycrystalline Ni films grown without the Fe seed layer. The epitaxial Ni film is expected to have a larger misfit strain and therefore a larger magneto-elastic anisotropy compared to the polycrystalline film, hence a larger PMA; we note, however, that there is a considerable out-of-plane remanence even for the polycrystalline Ni films. As a function of Ni thickness, the 20, 40 and 60 Å epitaxial Ni films are perpendicularly magnetized and show complete squareness ($M_r/M_s = 1$), indicating a strong perpendicular magnetic anisotropy. The reduced squareness and increased saturation field in the case of the 100 and 150 Å Ni films (with Fe seed layer) is associated with dominant in-plane easy axis. For Ni films grown using the Fe seed layer, the easy axis therefore changes from out-of-plane to in-plane between 60 and 100 Å Ni thickness (around 90 Å, as extrapolated from the perpendicular anisotropy constants for the 100 and 150 Å Ni films). This is similar to the transition thickness for Ni films grown on Cu/Si(001) which occurs between 100 and 140 Å (see figure 7).

Figure 6 shows the longitudinal MOKE curves for Cu/Ni/Cu/Fe/MgO with different Ni thicknesses. In this case, the 100 and 150 Å Ni film show a square in-plane easy axis loop. The hysteresis curves for the 20, 40 and 60 Å Ni films look at first sight unusual, but are understood as follows, taking into account that the polar Kerr effect is much stronger compared to the longitudinal Kerr effect: Ni films 20–60 Å thick are perpendicularly magnetized and an in-plane magnetic field leads to a gradual rotation of the magnetization

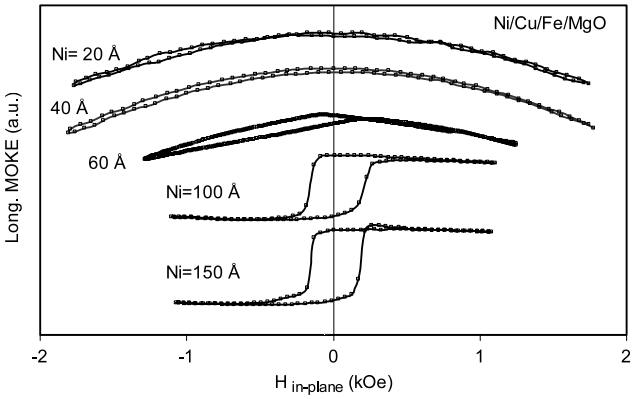

Figure 6. Longitudinal MOKE curves for Cu/Ni/Cu/Fe/MgO for the different Ni thicknesses.

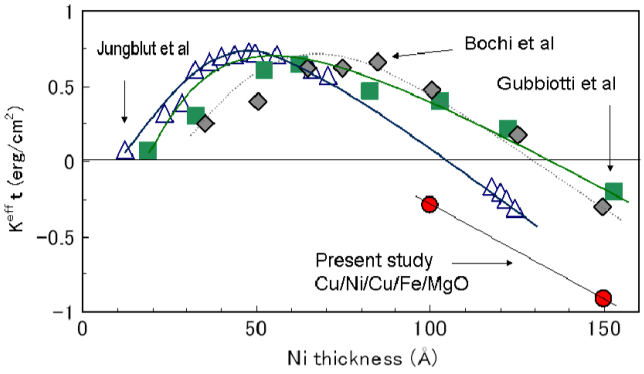

Figure 7. $t\,K_{\rm eff}$ versus Ni film thickness for Cu/Ni/Cu(001) films as reported by Jungblut *et al* [4] using ferromagnetic resonance (FMR), and for Cu/Ni/Cu/Si(001) films reported by Gubbiotti *et al* [28] (using Brillouin light scattering, BLS) and Bochi *et al* [28, 31] (from torque magnetometry measurements). Also shown are $t\,K_{\rm eff}$ for Cu/Ni/Cu/Fe/MgO(001) (present study). The lines are guides to the eye.

in-plane with increasing field strength; since the polar Kerr effect is dominant, we observe a reduced polar magnetization with increasing field strength. However, due to the large perpendicular magnetic anisotropy, magnetic saturation could not be reached with the maximum field available in the longitudinal MOKE configuration.

For a magnetic film with uniaxial anisotropy with a field applied along the hard axis direction, one expects [24]:

$$M_{\rm s}H = -2K_{u1}m - 4K_{u2}m^3$$

where K_{u1} (K_{u2}) is the first (second) order magnetic anisotropy constant, $K^{\rm eff} = K_{u1} + 2K_{u2}$ is the effective perpendicular magnetic anisotropy constant, m is the normalized component of the magnetization parallel to the applied field, and $M_{\rm s}$ is the saturation magnetization. This expression allows one to determine the perpendicular magnetic anisotropy constants for the in-plane magnetized films by fitting the polar MOKE loops (in the range $-0.95M_{\rm s} < M < 0.95M_{\rm s}$) to polynomial curves for the 100 and 150 Å Ni/Cu/Fe/MgO; the values of K_{u1} and K_{u2} were estimated assuming $M_{\rm s}$ to be the bulk value (483 emu cm^{-3} at RT) [25]. The values of $K_{\rm eff}$ obtained from the fits are plotted in figure 7, together with the values for the perpendicular magnetic anisotropy constant, $K_{\rm eff}$, of Ni as a function of film thickness reported in the literature for Cu/Ni/Cu(001) and Cu/Ni/Cu/Si(001). For Ni films grown on Cu/Si(001) above 140 Å Ni film thickness, in-plane magnetization is observed due to the dominant shape anisotropy (due to magnetic dipolar interactions). In the thickness range from about 20–140 Å, perpendicular magnetic anisotropy dominates, caused by a strong magneto-elastic anisotropy of the tensilely strained Ni film. For thicknesses below 20 Å, an in-plane magnetic anisotropy is found, suggested to be caused by a negative interface anisotropy [4, 8, 26, 27]. Qualitatively the same behaviour is observed for Ni films grown on Cu(001) and Cu/Si(001) films. It is found that $K^{\rm eff}$ for the Ni films on Cu/Fe/MgO follows a similar thickness dependence as that of the Ni/Cu/Si(001) films; the slightly smaller transition value between perpendicular to in-plane magnetization seems significant, however: Ni films grown on Cu(001) single crystals by Jungblut *et al* [4] also have a lower transition thickness than for Ni films grown on Cu/Si(001) [6, 28] (see also [29]). Residual strain in Cu/Si(001) could be one possibility, although recent experimental evidence does not support this [9]. One possible explanation may be the larger roughness of the Cu/Si(001) surface which may extend the coherent critical thickness by effectively increasing the contact area between the Cu and Ni surfaces. The differences in the magnetic behaviour of Ni films grown on Cu/Si(001) and Cu(001) single crystals are still not fully understood to date [29, 30].

In summary, the structure and magnetic properties of Cu/Ni/Cu/Fe/MgO(001) and Cu/Ni/Cu/MgO(001) thin films were investigated. The use of a thin Fe seed layer (5 Å) was demonstrated to be effective in achieving epitaxial growth of Ni/Cu films on Fe/MgO(001). Without the Fe seed layer the films grow polycrystalline, as previously found. The variation of the magnetic anisotropy of Cu/Ni/Cu/Fe/MgO with Ni thickness is found to be similar to that observed in the Cu/Ni/Cu/Si(001) system.

Acknowledgments

The financial support by the EPSRC is acknowledged. We are grateful to Heather Lawrence for her help in this project.

References

[1] Gradmann U and Müller J 1968 *Phys. Status Solidi* **27** 313
[2] Gradmann U and Müller J 1968 *J. Appl. Phys.* **39** 1379
[3] O'Brien W L, Droubay T and Tonner B P 1996 *Phys. Rev.* B **54** 9297
[4] Jungblut R, Johnson M T, aan de Stegge J, Reinders A and den Broeder F J A 1994 *J. Appl. Phys.* **75** 6424
[5] Rosenbusch P, Lee J Y, Lauhoff G and Bland J A C 1997 *J. Magn. Magn. Mater.* **172** 19
[6] Bochi G, Ballentine C A, Inglefield H E, Thompson C V, O'Handley R C and Hug H J 1995 *Phys. Rev.* B **52** 7311
[7] Bochi G, Hug H J, Paul D I, Moser A, Parashikov I, Güntherodt H-J and O'Handley R C 1995 *Phys. Rev. Lett.* **75** 1839
[8] Schulz B and Baberschke K 1994 *Phys. Rev.* B **50** 13467
[9] Vaz C A F, Steinmüller J, Moutafis C, Bland J A C and Babkevich A Y 2007 *Surf. Sci.* **601** 1377

[10] Martinez Boubeta C, Costa-Kraemer J L, Anguita J V, Cebollada A, Briones F, de Teresa J M, Morellon L, Ibarra M R, Guell F, Peiro F and Cornet A 2001 *Appl. Phys. Lett.* **79** 1655
[11] Parkin S S P, Kaiser C, Panchula A, Rice P M, Hughes B, Samant M and Yang S H 2004 *Nat. Mater.* **3** 862
[12] Yuasa S, Nagahama T, Fukushima A, Suzuki Y and Ando K 2004 *Nat. Mater.* **3** 868
[13] Zhou J B and Gustafsson T 1997 *Surf. Sci.* **375** 221
[14] Colonna S, Arcipreteb F, Balzarottib A, Fanfonib M, De Crescenzic M and Mobiliod S 2002 *Surf. Sci.* **512** L341
[15] Yang X and Perry S S 2002 *Surf. Sci. Lett.* **506** L261
[16] Mewes T, Rickart M, Mougin A, Demokritov S O, Fassbender J, Hillebrands B and Scheib M 2001 *Surf. Sci.* **481** 87
[17] Bland J A C, Padgett M J, Butcher R J and Bett N 1989 *J. Phys. E: Sci. Instrum.* **22** 308–12
[18] Daboo C, Bland J A C, Hicken R J, Ives A J R and Baird M J 1993 *Phys. Rev.* B **47** 11852
[19] Boubeta C M, Clavero C, Garcia-Martin J M, Armelles G, Cebollada G, Balcells L, Menendez J L, Peiro F, Cornet A and Toney M F 2005 *Phys. Rev.* B **71** 014407
[20] Kanaji T, Asano K and Nagata S 1973 *Vacuum* **23** 55
[21] Urano T and Kanaji T 1988 *J. Phys. Soc. Japan* **57** 3403
[22] Lee J, Lauhoff G, Tselepi M, Hope S, Rosenbusch P, Bland J A C, Dürr H A, van der Laan G, Schille J P and Matthew J A D 1997 *Phys. Rev.* B **55** 15103–7
[23] Lee J and Bland J A C 1997 *Surf. Sci.* **382** L672
[24] Sucksmith W and Thompson J E 1954 *Proc. R. Soc.* A **225** 362
[25] Lide D R 1995 *Handbook of Chemistry and Physics* 76th edn (Boca Raton, FL: CRC Press)
[26] Lauhoff G, Vaz C A F, Bland J A C, Lee J and Suzuki T 2000 *Phys. Rev.* B **61** 6805–10
[27] Baberschke K 2001 *Anisotropy in Magnetism* ed K Baberschke, M Donath and W Nolting (Berlin: Springer) p 27
[28] Gubbiotti G, Carlotti G, Ciria M and O'Handley R C 2002 *IEEE Trans. Magn.* **38** 2649
[29] Vaz C A F, Bland J A C and Lauhoff G 2008 *Rep. Prog. Phys.* **71** 056501
[30] Ney A, Poulopoulos P, Lenz K, Wende H and Baberschke K 2001 *Phys. Rev.* B **65** 024411
[31] Bochi G, Ballentine C A, Inglefield H E, Thompson C V and O'Handley R C 1996 *Phys. Rev.* B **53** R1729